Communication

Snow Parameters Inversion from Passive Microwave Remote Sensing Measurements by Deep Convolutional Neural Networks

Heming Yao [1,†], Yanming Zhang [2,†] [iD], Lijun Jiang [2], Hong Tat Ewe [3] and Michael Ng [1,*]

[1] Department of Mathematics, The University of Hong Kong, Pokfulam Road, Hong Kong 999077, China
[2] Department of Electrical and Electronic Engineering, The University of Hong Kong, Pokfulam Road, Hong Kong 999077, China
[3] Department of Electrical and Electronic Engineering, Universiti Tunku Abdul Rahman, Perak 31900, Malaysia
* Correspondence: mng@maths.hku.hk
† These authors contributed equally to this work.

Abstract: This paper proposes a novel inverse method based on the deep convolutional neural network (ConvNet) to extract snow's layer thickness and temperature via passive microwave remote sensing (PMRS). The proposed ConvNet is trained using simulated data obtained through conventional computational electromagnetic methods. Compared with the traditional inverse method, the trained ConvNet can predict the result with higher accuracy. Besides, the proposed method has a strong tolerance for noise. The proposed ConvNet composes three pairs of convolutional and activation layers with one additional fully connected layer to realize regression, i.e., the inversion of snow parameters. The feasibility of the proposed method in learning the inversion of snow parameters is validated by numerical examples. The inversion results indicate that the correlation coefficient (R^2) ratio between the proposed ConvNet and conventional methods reaches 4.8, while the ratio for the root mean square error (RMSE) is only 0.18. Hence, the proposed method experiments with a novel path to improve the inversion of passive microwave remote sensing through deep learning approaches.

Keywords: machine learning; deep convolutional neural networks (CNNs); passive microwave remote sensing (PMRS); inversion; dense medium radiative transfer (DMRT)

1. Introduction

As an important informative indicator for climate change, snowpack presents both the surface energy and water balance in a certain region [1,2]. Passive microwave remote sensing (PMRS) data have been widely employed to analyze snowpack because passive microwave remote sensing schemes can be applied in various weather and can penetrate clouds and snow [3,4]. Generally, the analysis and retrieval of snowpack by passive microwave measurements is based on the physical scattering model, which can produce both backscatter and brightness temperature measured from the physical parameters of the snowpack [5–8]. In this inversion process, multiple scattering in passive microwave remote sensing problems can be a dominant effect because the relation between remote sensing measurements and the medium parameters is highly nonlinear [5–8]. In the last decades, the research related to the inversion algorithm to obtain parameters of the snowpack by PMRS data has developed rapidly [9,10]. However, these conventional inversion methods, such as the conventional iterative method [11], Empirical formulas method [12] and artificial neural network (ANN) method [13,14], often make the process computationally expensive and even ill-posed [11–15].

The application of machine learning (ML) in advanced computational electromagnetics, such as object monitoring [16], electromagnetic simulation [17–21] and field-circuit

cosimulations [22,23], was initiated a long time ago. Machine learning methods aim to derive the potential mapping disciplinarian by employing the same pattern's training data and predicting the new output. Due to recent blooming learning technologies, the convolutional neural network (ConvNet) [24,25] has become one of the most significant methods in deep learning-based applications, such as imaging processes [24,25]. Various rough surface theory methods have been widely studied and applied in the simulation of snow [26,27]. However, the inverse problem still faces the challenge of nonlinearity and high computational complexity, which is still an open issue. In fact, machine learning methods such as conventional multiple layers artificial neural network (ANN) technique [14,28] and support vector machine [29], have been used to inverse parameters of the snowpack based on PMRS data. However, the inversion based on conventional machine learning methods suffers from limited accuracy, even with complex structure [21,28,29].

In this paper, we propose the employment of a deep ConvNet for inverting snow parameters (the thickness t and the temperature T of the snowpack) from passive microwave remote sensing measurements. The basic process is to use the input-output pairs generated by the scattering simulation model to train the proposed deep ConvNet. Once the ConvNet is trained, it can invert snow parameters (the thickness t and the temperature T of the snowpack) speedily and accurately from the measurements. The advantages of the proposed method are: (1) High accuracy: the proposed inverse ConvNet model can provide results with high accuracy, compared with support vector machine and conventional artificial neural networks trained for the inversion of snow parameters from passive microwave remote sensing [21,28,29]; (2) Simplicity: the training of the proposed deep ConvNet is merely based on the data simulated numerically using computational electromagnetic method, instead of using experimental measurement data; (3) High Noise Tolerance: the proposed ConvNet is of strong anti-interference and its accuracy is high, even though significant interference is added. Compared to the conventional artificial neural networks (ANNs) and the support vector machine (SVM) method [21,28,29], the proposed deep ConvNet can more efficiently map the relations between inputs and outputs, mainly by the convolutional layer and activation layer [24,25]. Consequently, the correlation coefficient (R^2) of the ConvNet method can be about 4.8 times as large as that of SVM for inversing T. Meanwhile, the root mean square error (RMSE) of the ConvNet method can be only 0.18 of the ANN method for inversing t. A specific comparison between different approaches is provided in Section 3.

The remainder of this article is organized as follows: In Section 2, the passive microwave remote sensing, the snowpack model, and dense media radiative transfer (DMRT) model formulation is briefly reviewed, followed by a description of the proposed deep ConvNet structure. Then, the training process of the proposed ConvNet for snow parameters inversion is described. In Section 3, numerical examples are provided to present the validity and precision of the proposed method, which are also compared with the results obtained by the conventional artificial neural network. Finally, the conclusion is given in Section 4.

2. Formulations

2.1. Snow Model and DMRT Model for PMRS

The model of the microwave emission behaviour for multilayer snowpacks is shown in Figure 1. It has been demonstrated that dense medium radiative transfer (DMRT) shows high validity and efficiency [30]. Thus, the input-output pairs for training ConvNet are generated by utilizing DMRT based on the quasicrystalline approximation (QCA) in this research. The DMRT formulas for PMRS could be simplified by amending these formulas for active microwave remote sensing because of the azimuthal symmetry. The standard formulation of the DMRT in the multilayer dielectric medium can be expressed as:

$$\cos\theta \frac{d}{dz} \boldsymbol{I}(\theta, z) = -\kappa_e \boldsymbol{I}(\theta, z) + \boldsymbol{S}(\theta, z) + \kappa_a \boldsymbol{T}$$

$$-\cos\theta \frac{d}{dz} \boldsymbol{I}(\pi - \theta, z) = -\kappa_e \boldsymbol{I}(\pi - \theta, z) + \boldsymbol{W}(\theta, z) + \kappa_a \boldsymbol{T}$$

(1)

where

$$\boldsymbol{S}(\theta, z) = \int_0^{2\pi} d\theta' \sin\theta' \left[\boldsymbol{P}(\theta, \phi; \theta', \phi' = 0) \cdot \boldsymbol{I}(\theta', z) + \right.$$

$$\left. \boldsymbol{P}(\theta, \phi; \pi - \theta', \phi' = 0) \cdot \boldsymbol{I}(\pi - \theta', z) \right]$$

$$\boldsymbol{W}(\theta, z) = \int_0^{2\pi} d\theta' \sin\theta' \left[\boldsymbol{P}(\pi - \theta, \phi; \theta', \phi' = 0) \cdot \boldsymbol{I}(\theta', z) + \right.$$

$$\left. \boldsymbol{P}(\pi - \theta, \phi; \pi - \theta', \phi' = 0) \cdot \boldsymbol{I}(\pi - \theta', z) \right]$$

(2)

Herein, $\boldsymbol{I}(\theta, z)$ denotes the specific intensity of horizontal and vertical polarizations, which is independent of the azimuthal angle ϕ. κ_e and κ_a are the extinction coefficient and absorption coefficient respectively. The phase matrix $\boldsymbol{P}$ is simplified by using 1–2 frames [28,31]. $\boldsymbol{T}$ means the transmissivity matrices from ground to snow and from snow to snow. Combing the boundary conditions [30], these differential equations could be analyzed in the whole layers. The details of solving these equations could be found in [30,32], and it is demonstrated that the results of the multilayer QCA/DMRT agree well with the CLPX ground measurement [32]. In this paper, the input medium physical parameters of DMRT are: (1) snowpack thickness t; (2) physical temperature T of the snowpack. From these parameters, the brightness temperature B_v in vertical polarization and B_h in horizontal polarization at various observation angles could be simulated by the above model.
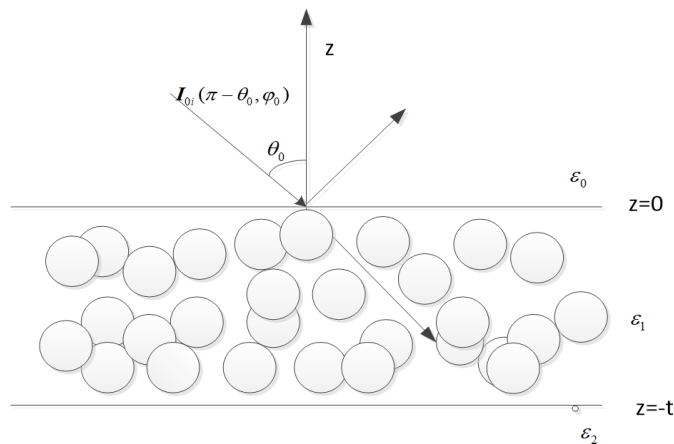

Figure 1. Model microwave emission behavior for multilayer snowpacks.

2.2. Deep ConvNet Architecture

In our approach, the ConvNet model is utilized to inverse the thickness t and the temperature T of the snowpack from its corresponding brightness temperature B_v in vertical polarization and B_h in horizontal polarization. These arrays of brightness temperature B_v in vertical polarization and B_h in horizontal polarization can be measured by passive microwave remote sensing based on DMRT numerical simulation. In fact, the brightness temperature B_v and B_h indicate the feature information of snow [30,32]. In the training process, the thickness t and the temperature T of the snowpack are utilized as outputs to our deep ConvNets. Their corresponding brightness temperature B_v and B_h are employed as the inputs in the proposed framework.

Typical ConvNets [24,25] consist of four types of layers: input layers, convolutional layers, pooling layers and fully-connected layers. By stacking these layers together, the proposed ConvNet architecture is formed. As the typical deep neural networks, ConvNet can make use of data in the form of spatially focused images [21,33]. The specific architecture of the proposed ConvNet is presented in Figure 2. Because of the strong capability of

ConvNet, our approach can convert the brightness temperature B_v in vertical polarization and B_h in horizontal polarization with more substantial interference into the corresponding thickness t and the temperature T of the snowpack.
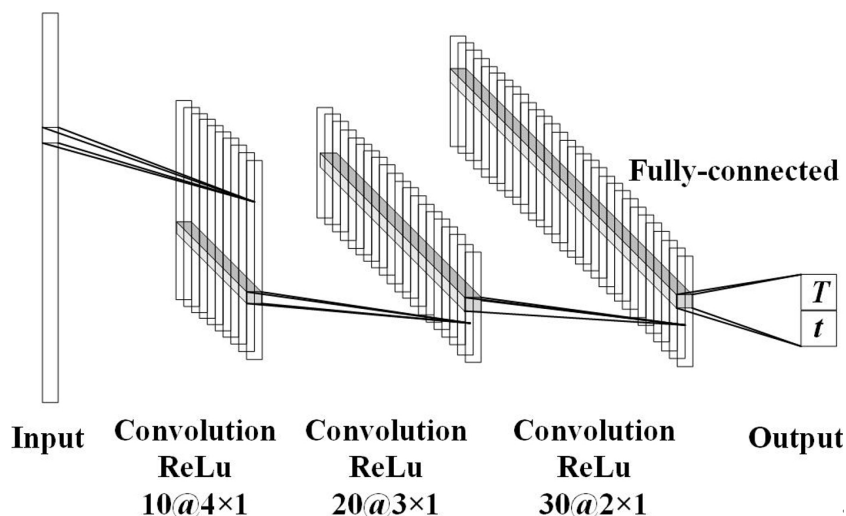

Figure 2. ConvNet architecture for the inversion of snow parameters.

2.3. Data Preparation and ConvNet Training

Considering the requirement for the massive number of input training data is challenging to yield via actual observations, we employ numerical simulation to obtain the input data for the training process of the proposed ConvNet. By PMRS of snowpack based on DMRT numerical simulation, both the brightness temperature B_v in vertical polarization and B_h in horizontal polarization are measured under incident angle θ_{inc} evenly distributed within $[6°, 75°]$, and form the 'field-data' $[B_v, B_h]$ with the size of 70×2, as is presented in Figure 3. Considering the interference in the actual application scenario, the random noise with signal-to-noise ratio (SNR) up to 0 dB is added to the measured the brightness temperature 'field-data' $[B_v, B_h]$ to form the input training data, while $[t, T]$ of the snowpack is utilized as outputs to our deep ConvNets.

The procedures of producing training data are formulated into the following two steps: (1) the brightness temperature is firstly calculated from the different thickness t and the temperature T of the snowpack by DMRT model, where the values of t and T are within $t \in \{16\,\text{cm}, 18\,\text{cm}, \ldots, 44\,\text{cm}\}$ and $T \in \{250\,\text{K}, 252\,\text{K}, \ldots, 270\,\text{K}\}$, respectively. (2) the random noise with signal-to-noise ratio (SNR) up to -10 dB is added to the brightness temperature computed in (1) to form one group of input of the proposed ConvNet, while the output is the corresponding t and T. 5000 groups of the brightness temperature 'field data' $[B_v, B_h]$ with noise and the corresponding accurate $[t, T]$ are used as inputs and outputs of the proposed ConvNet. All simulation computation is done on snow-covered ground with the flat bottom surface and with known parameters: grain diameter is 0.1 cm, snow density in gm/cc is 0.276, QCA stickiness parameter is 0.1, the ground temperature is 270 K and the frequency of measurement microwave is 18.7 GHz.
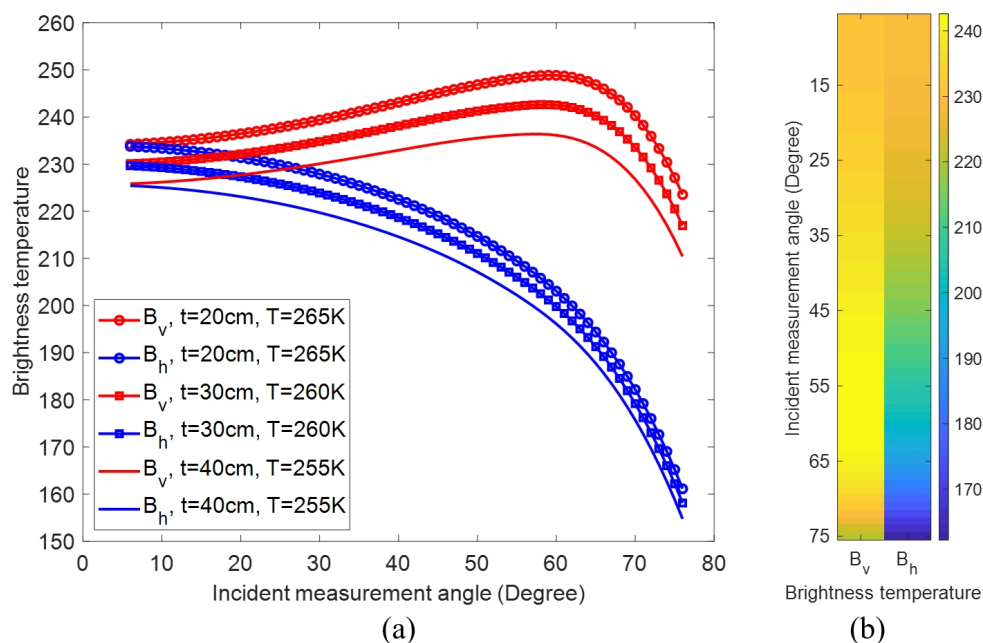
Figure 3. (**a**) the brightness temperature B_v in vertical polarization and B_h in horizontal polarization with $t = 30$ cm and $T = 260$ K; (**b**) the 'field-data' $[B_v, B_h]$ as the input of ConvNet.

As shown in Figure 2, the convolutional and activation layer units operate to grasp the input characteristics. In the convolutional layer, we pick the filters (kernel) with a one-dimension (1D) size. Such a 1D kernel has broadly been used in processing text natural language and predicting stock [34,35]. Table 1 presents the number of Convolutional layers and kernel. In addition, the size and the stride of the kernel are detailed. For the output, i.e., the predicted thickness t and the temperature T of the snowpack, a fully-connected layer is adopted for the prediction, which is fed by the activation layer unit. Herein, the loss function is defined by the half mean squared error between the actual label and the predicted one, i.e., the output of the fully-connected layer. Our proposed approach is benchmarked via the Deep Learning Toolbox in Matlab 2018b [36]. Here, the Adaptive Moment Estimation (Adam) optimizer is selected to optimize the half mean squared error loss function. This is because, compared with other optimizers like Stochastic Gradient Descent (SGD) [37], the Adam optimizer can navigate through the loss surface more successfully. Notably, the learning rate, a hyper-parameter in the proposed framework, can be used to control training error. We set the learning rate as 0.01. In addition, to avoid the over-fitting issue, L2 regularization is used for the improvement of prediction accuracy [38]. All the training is implemented with the full batch.

Table 1. ConvNet architecture.

Type	Filter Number	Filter Size	Stride	Input Size	Output Size
Convolution	10	4×1	[2 1]	$70 \times 2 \times 1$	$34 \times 2 \times 10$
ReLu				$34 \times 2 \times 10$	$34 \times 2 \times 10$
Convolution	20	3×1	[2 1]	$34 \times 2 \times 10$	$16 \times 2 \times 20$
ReLu				$16 \times 2 \times 20$	$16 \times 2 \times 20$
Convolution	30	2×1	[2 1]	$16 \times 2 \times 20$	$8 \times 2 \times 30$
ReLu				$8 \times 2 \times 30$	$8 \times 2 \times 30$
Fully-connected					
Regression				480	2

3. Numerical Examples

In this section, the trained Convnet is used to predict the thickness t and the temperature T of the snowpack. In total, 150 groups of the measured brightness temperature 'field-data' $[B_v, B_h]$ with (SNR = 0 dB) noise calculated by different the thickness and the temperature $[t, T]$ of the snowpack were used as inputs of our trained ConvNet, where the values of t and T are within $t \in \{17\,\text{cm}, 19\,\text{cm}, \dots, 43\,\text{cm}\}$ and $T \in \{251\,\text{K}, 253\,\text{K}, \dots, 269\,\text{K}\}$, respectively.

The comparison of the prediction of t and T and the actual values is presented in Figure 4a,b respectively. It can be indicated that the predicted data points of both t and T are closely distributed around the straight line Y = X. Evidently, the proposed ConvNet can effectively realize inversion of the thickness t and the temperature T of the snowpack even under big interference. According to Figure 4a, the correlation coefficient (R^2) between the predicted and actual t is even 0.9964, while the root mean square error (RMSE) of them is only 0.3869. Thus, despite noise, the proposed ConvNet can predict the thickness t under much high accuracy.

Figure 4b shows that the change tendency of the snow temperature T in Figure 4b is similar to that of the snow thickness t in Figure 4a. From Figure 4b, the correlation coefficient (R^2) between the predicted T and the actual T is 0.8380, while the root mean square error (RMSE) of two sets of T is 1.7873. The inversion prediction of T closed to the scope of trained values has more error than the prediction away from the scope of trained values. This is simply because the predicted values are limited in the scope of trained values. As the values of inverted parameter are close to the end of the scope, those inaccurately predicted values shift toward the other end [21]. In our deep ConvNet approach, the thickness t and the temperature T can be inverted simultaneously at the nearly equivalent accuracy by the same deep network rather than two separated networks.
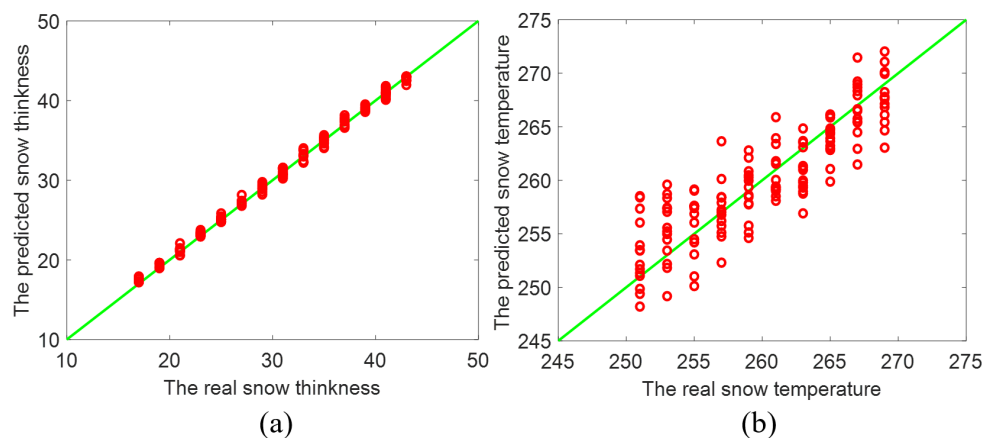

Figure 4. Inverted result of (**a**) the thickness and (**b**) the temperature of the snowpack by the proposed ConvNet method.

Moreover, we compare the ConvNet inversion result of t and T with that predicted from conventional artificial neural network (ANN) [28], to demonstrate the capability of our deep ConvNet. Conventional ANNs depend on neural unit and hidden layer to fit the relationship between input and output, and have to make use of a large number of neural units to handle the relatively complicated relationship between input and output [28]. The architecture of used ANN has three layers: input, hidden-layer, and output layer. There are 20 hidden-layer units of hyperbolic tangent basis function. The BPNN is implemented using Matlab 2018b with Deep Learning Toolbox [36]. For this case, the increase of ANN hidden layer or its units do not lead to the great improvement of accuracy, but leads to the increase of unexpected computation cost and degrades its efficiency. As shown in Figure 5a,b, the correlation coefficient (R^2) between the predicted t and actual t is 0.9321 while R^2 between two sets of T is as small as 0.3332. Besides, the root mean square error

(RMSE) of the predicted t and actual t arrives at only 2.1036, and RMSE of two sets of T reaches 3.5625. Therefore, the estimation accuracy of the ConvNet is higher than that of the conventional ANN by comparing Figures 4 and 5.

Furthermore, the SVM method is also used to invert the t and T [21,29]. As is presented in Figure 6a,b, R^2 between the predicted t and actual t is 0.9667, while RMSE of them is as small as 0.6232. Besides, R^2 and RMSE between two sets of T are 0.1749 and 6.4291, respectively. Thus, as is shown in Figure 6, the estimation accuracy of the SVM is undoubtedly lower than both the proposed ConvNet and conventional ANN. In addition, both the proposed deep ConvNet and conventional ANN can simultaneously invert the t and T, while the SVM model has to make use of two different models to undertake the inversion.
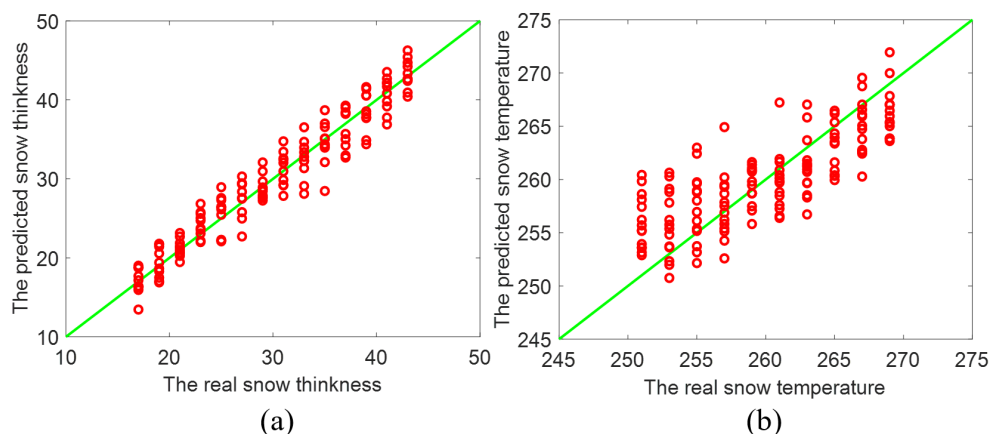

(a) (b)

Figure 5. Inverted result of (**a**) the thickness and (**b**) the temperature of the snowpack by the conventional ANN method [14,28].
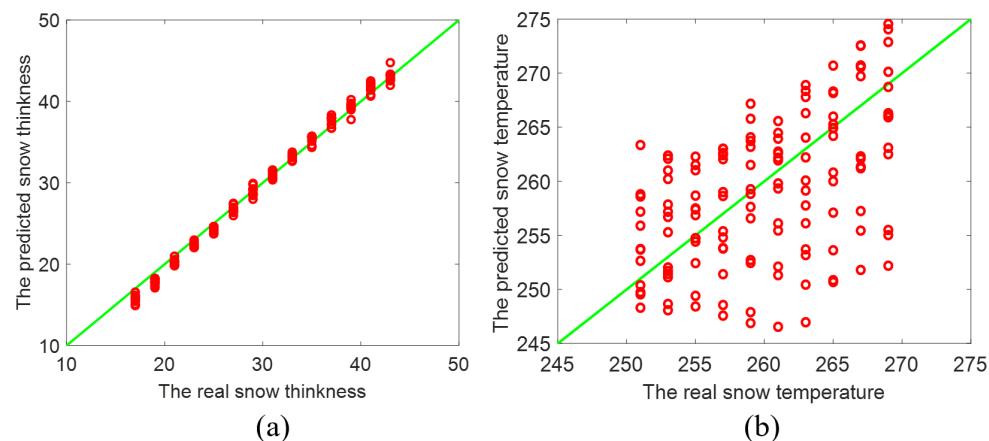

(a) (b)

Figure 6. Inverted result of (**a**) the thickness and (**b**) the temperature of the snowpack by the SVM method [21,29].

As presented in Figures 3–6, the proposed deep ConvNet can utilize PMRS data with significant noise to extract the features and retrieve t and T. The deep ConvNet employs data in the form of spatially focused images to discover recognition and imaging [21,26]. Thus, despite huge noise and abstract PMRS data, the performance of the deep ConvNet could be much better than the other two methods. The overall performance of the three methods is also shown in the Table 2. It is evident that the proposed deep ConvNet can inverse t and T with the largest R^2 and the smallest RMSE among the three methods. While R^2 of the ConvNet method can be about 4.8 times as large as that of SVM for inversing T, RMSE of the ConvNet method can be only 18% of that of ANN method for inversing t. In this study, we have focused on thickness and temperature, while other parameters could be added to the proposed deep ConvNets. We aim to do this in future studies. Also, extremes

of the working ranges of thickness and temperature as well as the lower boundary of SNR in the anti-interference simulation could be included in future research.

Table 2. Performance Comparison.

		R^2	RMSE	$\frac{R^2_{DConvNet}}{R^2}$	$\frac{RMSE_{DconvNet}}{RSME}$
	DConvNet	**0.9964**	**0.3869**		
t	ANN	0.9321	2.1036	1.0690	0.1839
	SVM	0.9667	0.6232	1.0307	0.6208
	DConvNet	**0.8380**	**1.7873**		
T	ANN	0.3332	3.5625	2.5150	0.5017
	SVM	0.1749	6.4291	4.7913	0.2780

4. Conclusions

To sum up, a novel inversion method is proposed to extract the layer thickness and temperature of snowpack by using the deep convolutional neural network (ConvNet). The proposed ConvNet consists of three pairs of convolutional and activation layers, following one additional fully connected layer to the inverse of snow parameters. The training of the proposed deep ConvNet is based on simulated data obtained through a dense medium radiative transfer equation (DMRT). The training data also considers the possible interference in a real application scenario. The trained deep ConvNet can inverse the layer thickness and temperature of snowpack within an acceptable accuracy range, which indicates its capacity for anti-interference. Numerical examples indicate the validity of the proposed deep ConvNet for the inversion of parameters of the snowpack. Compared with the conventional artificial neural network and support vector machine, the trained ConvNet can predict the result with higher accuracy. The proposed ConvNet method opens a novel path for deep learning application to passive microwave remote sensing.

References

1. Zhang, T.J. Influence of the seasonal snow cover on the ground thermal regime: An overview. *Rev. Geophys.* **2005**, *43*, 43–66. [CrossRef]
2. Frei, A.; Robinson, D.A. Northern Hemisphere snow extent: Regional variability 1972–1994. *Int. J. Climatol.* **1999**, *19*, 1535–1560. [CrossRef]

3. Foster, J.L.; Hall, D.K.; Chang, A.T.C.; Rango, A. An overview of passive microwave snow research and results. *Rev. Geophys. Space Phys.* **1984**, *22*, 195–208. [CrossRef]

4. Koike, T.; Suhama, T. Passive-microwave remote sensing of snow. *Ann. Glaciol.* **1993**, 18, 305–308. [CrossRef]

5. Tan, S.; Zhu, J.; Tsang, L.; Nghiem, S.V. Full wave simulation of snowpack applied to microwave remote sensing of sea ice. In Proceedings of the 2017 IEEE International Geoscience and Remote Sensing Symposium (IGARSS), Fort Worth, TX, USA, 23–28 July 2017; pp. 1380–1383.

6. Mätzler, C.; Wiesmann, A. Extension of the microwave emission model of layered snowpacks to coarse-grained snow. *Remote Sens. Environ.* **1999**, *70*, 317–325. [CrossRef]

7. Zhu, J.; Tan, S.; King, J.; Derksen, C.; Lemmetyinen, J.; Tsang, L. Forward and Inverse Radar Modeling of Terrestrial Snow Using SnowSAR Data. *IEEE Trans. Geosci. Remote Sens.* **2018**, *56*, 7122–7132. [CrossRef]

8. Singh, R.; Gan, T.Y. Retrieval of snow water equivalent using passive microwave brightness temperature data. *Remote Sens. Environ.* **2000**, *74*, 275–286. [CrossRef]

9. Solberg, R.; Rudjord, O.; Salberg, A.B.; Killie, M.A. A multi-sensor multitemporal algorithm for snow cover extent retrieval from optical and passive microwave data. In Proceedings of the 7th EARSeL Workshop on Land Ice and Snow, Bern, Switzerland, February 2014; pp. 3–6.

10. Che, T.; Dai, L.; Zheng, X.; Li, X.; Zhao, K. Estimation of snow depth from passive microwave brightness temperature data in forest regions of northeast China. *Remote Sens. Environ.* **2016**, *183*, 334–349. [CrossRef]

11. Tanikawa, T.; Li, W.; Kuchiki, K.; Aoki, T.; Hori, M.; Stamnes, K. Retrieval of snow physical parameters by neural networks and optimal estimation: Case study for ground-based spectral radiometer system. *Opt. Express* **2015**, *23*, A1442–A1462. [CrossRef]

12. Hallikainen, M.T.; Jolma, P. Comparison of algorithms for retrieval of snow water equivalent from Nimbus-7 SMMR data in Finland. *IEEE Trans. Geosci. Remote Sens.* **1992**, *30*, 124–131. [CrossRef]

13. Davis, D.T.; Chen, Z.; Tsang, L.; Hwang, J.-N.; Chang, A.T.C. Retrieval of snow parameters by iterative inversion of a neural network. *IEEE Trans. Geosci. Remote Sens.* **1993**, *31*, 842–851. [CrossRef]

14. Tedesco, M.; Pulliainen, J.; Takala, M.; Hallikainen, M.; Pampaloni, P. Artificial neural network-based techniques for the retrieval of SWE and snow depth from SSM/I. *Remote Sens. Environ.* **2004**, *90*, 76–85. [CrossRef]

15. Pulliainen, J.; Hallikainen, M. Retrieval of regional snow water equivalent from space-borne passive microwave observations. *Remote Sens. Environ.* **2001**, *75*, 76–85. [CrossRef]

16. Zhang, H.H.; Chen, R.S. Coherent processing and superresolution technique of multi-band radar data based on fast sparse Bayesian learning algorithm. *IEEE Trans. Antennas Propag.* **2014**, *62*, 6217–6227. [CrossRef]

17. Yao, H.; Jiang, L.; Qin, Y. Machine learning based method of moments (ML-MoM). In Proceedings of the 2017 IEEE International Symposium on Antennas and Propagation and USNC/URSI National Radio Science Meeting, San Diego, CA, USA, 9–14 July 2017.

18. Shan, T.; Tang, W.; Dang, X.W.; Li, M.K.; Yang, F.; Xu, S.H.; Wu, J. Study on a Poisson's Equation Solver Based On Deep Learning Technique. *arXiv* **2017**, arXiv:1712.05559.

19. Yao, H.M.; Jiang, L. Machine-Learning-Based PML for the FDTD Method. *IEEE Antennas Wirel. Propag. Lett.* **2019**, *18*, 192–196. [CrossRef]

20. Yao, H.M.; Li, M.; Jiang, L. Applying Deep Learning Approach to the Far-Field Subwavelength Imaging Based on Near-Field Resonant Metalens at Microwave Frequencies. *IEEE Access* **2019**, *7*, 63801–63808. [CrossRef]

21. Song, T.; Kuang, L.; Han, L.; Wang, Y.; Liu, Q.H. Inversion of Rough Surface Parameters From SAR Images Using Simulation-Trained Convolutional Neural Networks. *IEEE Geosci. Remote Sens. Lett.* **2018**, *15*, 1130–1134. [CrossRef]

22. Zhang, H.H.; Yao, H.M.; Jiang, L.J. Embedding the behavior macromodel into TDIE for transient field-circuit simulations. *IEEE Trans. Antennas Propag.* **2016**, *64*, 3233–3238. [CrossRef]

23. Zhang, H.H.; Jiang, L.J.; Yao, H.M.; Zhang, Y. Transient heterogeneous electromagnetic simulation with DGTD and behavioral macromodel. *IEEE Trans. Electromagn. Compat.* **2017**, *59*, 1152–1160. [CrossRef]

24. Krizhevsky, A.; Sutskever, I.; Hinton, G. ImageNet classification with deep convolutional neural networks. *Commun. ACM* **2017**, *60*, 84–90. [CrossRef]

25. Zhang, Y.; Zhao, D.; Sun, J.; Zou, G.; Li, W. Adaptive Convolutional Neural Network and Its Application in Face Recognition. *Neural Process. Lett.* **2015**, *43*, 389–399. [CrossRef]

26. Zhang, Y.; Xu, G.; Zheng, Z. Terahertz waves propagation in an inhomogeneous plasma layer using the improved scattering-matrix method. *Waves Random Complex Media* **2021**, *31*, 2466–2480. [CrossRef]

27. Capelli, A.; Kapil, J.C.; Reiweger, I.; Or, D.; Schweizer, J. Speed and attenuation of acoustic waves in snow: Laboratory experiments and modeling with Biot's theory. *Cold Reg. Sci. Technol.* **2016**, *125*, 1–11. [CrossRef]

28. Tsang, L.; Chen, Z.; Oh, S.; Marks, R.J.; Chang, A.T.C. Inversion of snow parameters from passive microwave remote sensing measurement by a neural network trained with a multiple scattering model. *IEEE Trans. Geosci. Remote Sens.* **1992**, *30*, 1015–1024. [CrossRef]

29. Liang, J.; Liu, X.; Huang, K.; Li, X.; Shi, X.; Chen, Y.; Li, J. Improved snow depth retrieval by integrating microwave brightness temperature and visible/infrared reflectance. *Remote Sens. Environ.* **2015**, *156*, 500–509. [CrossRef]

30. Liang, D.; Xu, X.; Tsang, L.; Andreadis, K.M.; Josberger, E.G. The effects of layers in dry snow on its passive microwave emissions using dense media radiative transfer theory based on the quasicrystalline approximation (QCA/DMRT). *IEEE Trans. Geosci. Remote Sens.* **2008**, *46*, 3663–3671. [CrossRef]

31. Tan, S.; Chang, W.; Tsang, L.; Lemmetyinen, J.; Proksch, M. Modeling both active and passive microwave remote sensing of snow using dense media radiative transfer (DMRT) theory with multiple scattering and backscattering enhancement. *IEEE J. Sel. Top. Appl. Earth Obs. Remote Sens.* **2015**, *8*, 4418–4430. [CrossRef]

32. Tsang, L.; Kong, J.A.; Shin, R.T. *Theory of Microwave Remote Sensing*; Wiley: Hoboken, NJ, USA, 1985.

33. Zhou, Y.; Wang, H.; Xu, F.; Jin, Y. Polarimetric SAR Image Classification Using Deep Convolutional Neural Networks. *IEEE Geosci. Remote Sens. Lett.* **2016**, *13*, 1935–1939. [CrossRef]

34. Ding, X.; Zhang, Y.; Liu, T.; Duan, J. Deep learning for event-driven stock prediction. In Proceedings of the 24th International Conference on Artificial Intelligence (IJCAI'15), Buenos Aires, Argentina, 25–31 July 2015.

35. Tymoshenko, K.; Bonadiman, D.; Moschitti, A. Convolutional neural networks vs. convolution kernels: Feature engineering for answer sentence reranking. In Proceedings of the NAACL-HLT, San Diego, CA, USA, 12–17 June 2016; pp. 1268–1278.

36. Kim, P. *MATLAB Deep Learning*; Springer: New York, NY, USA, 2017.

37. Kingma, D.P.; Ba, J.L. Adam: A method for stochastic optimization. *Proc. Int. Conf. Learn. Represent.* **2015**, 1–41. [CrossRef]

38. Ng, A.Y. Feature Selection L1 vs. L2 Regularization and Rotational Invariance. In Proceedings of the Twenty-First International Conference on Machine Learning, Banff, AB, Canada, 4–8 July 2004; pp. 78–86.